JOURNAL OF MATERIALS SCIENCE 24 (1989) 3707–3711

High temperature oxidation of Ni_2AlTi

C. C. LEE, P. SHEN
Institute of Materials Science and Engineering, National Sun Yat-Sen University, Kaohsiung, Taiwan

The isothermal oxidation process in bulk and powdered Ni_2AlTi ($L2_1$ structure) has been studied in the temperature range of 600 to 1200° C in air by means of X-ray diffraction and scanning electron microscopy. At 900 and 1200° C, the transient oxides, NiO and TiO_2 were formed in the initial stage on the outer surface. Subsequent oxidation was dominated by outward diffusion of aluminium, resulting in the formation of a Ni_3Ti layer beneath an internal precipitation layer containing Al_2O_3–$NiAl_2O_4$ aggregates, $NiTiO_3$ and Ni_3Ti. Formation of $NiTiO_3$ and $NiAl_2O_4$ at the expense of NiO, TiO_2 and Al_2O_3 indicated the reaction among constituent oxides also occurred in the late stage of oxidation at 900 and 1200° C. Only NiO and TiO_2 were identified in specimens oxidized at 600° C up to 24 h. The oxidation rate of Ni_2AlTi is of the same order of magnitude as the dilute γ-NiAl alloy at 1200° C.

1. Introduction

Aluminized coatings prepared on nickel-based superalloys by the pack cementation method provide better protection against high temperature oxidation and hot corrosion than do the uncoated substrates [1–4]. It was generally accepted that the interdiffusion between aluminium and nickel resulted in a β-NiAl phase on the alloy surface which improved both the hot corrosion and the oxidation resistance [1, 2, 5]. According to metallographic, compositional and X-ray diffraction studies [1–5], high temperature oxidation resulted in the formation of the sesquioxide layer which resisted further oxidation of the aluminized coatings on superalloys. A recent transmission electron microscopy (TEM) study of the oxidation products of the aluminized coatings on Rene 80 indicated that the cubic oxides (RO and R_3O_4) and the sesquioxide (R_2O_3), where R represents cations, have preferred orientation relationships to the gamma phase initially. However, such crystallographic relationships disappeared when the oxide particles were greater than a certain critical size [6]. Gamma phase, gamma prime phase and Ni_2Al phase were formed by the degradation of the beta phase in the coating and had preferred orientation relationships to the beta phase [6].

Recent scanning transmission electron microscopy (STEM) studies of the aluminized coatings on the nickel-based superalloys of René 80, IN713LC and MAR-M247 showed that the beta matrix in diffusion zone may not necessarily be of B2 (NiAl) structure but can also be of $L2_1$ (Ni_2AlTi) structure depending on the titanium content of the alloy [7, 8]. The high temperature creep study of polycrystalline Ni_2AlTi [9] found that the creep strength of Ni_2AlTi is about three times that of NiAl. The deformation behaviour of single- and polycrystalline specimens of Ni_2AlTi were tested in compression in the temperature range 923 to 1283° K and the operative slip systems characterized [10]. Since NiAl is weak in high temperature creep, Ni_2AlTi could be an alternative coating material for use in high-temperature technology [10], it is, therefore, of interest to evaluate the oxidation resistance of Ni_2AlTi phase. Although the formation of TiO_2 was known to decrease the oxidation resistance of René 80 [5, 11], the high-temperature oxidation process of the stoichiometric Ni_2AlTi compound was not reported. The purposes of the present study are to characterize the crystal structures of the oxides and the retrograded metal phase during oxidation of Ni_2AlTi and to detect the sequence of formation of these phases by X-ray diffraction and scanning electron microscopy (SEM).

2. Experimental procedure

The Ni_2AlTi alloy was prepared from electrolytic nickel, aluminium and titanium by arc melting in argon. The bulk samples about $10 \times 5 \times 3\,mm^3$ in size were used for the oxidation test after polishing through alumina powder (0.05 μm in size) and rinsing with water, methyl alcohol and benzene. The resistance-heating furnace was preheated to desired temperature and the bulk samples were put in for isothermal (900 and 1200° C) oxidation treatment for 1 to 30 min in air. The samples were then cooled outside the furnace and polished for cross-sectional study by SEM (JEOL, JSM-35CF operating at 25 kV) coupled with energy dispersive X-ray (EDX) analysis. The distribution of phases was studied by sequential X-ray diffractions (Cu Kα) on the polished surface at a distance of 0, 10, 20 and 30 μm from the original outer surface. Alternatively Ni_2AlTi powder, mechanically ground from bulk Ni_2AlTi by mortar and pestle to less than 60 μm in size, was isothermally (600, 900 and 1200° C) oxidized for 5 sec to 1440 min using the same methods as the bulk samples. The oxidized powders were also studied by X-ray diffraction to identify the sequential formation of oxides.

0022–2461/89 $03.00 + .12

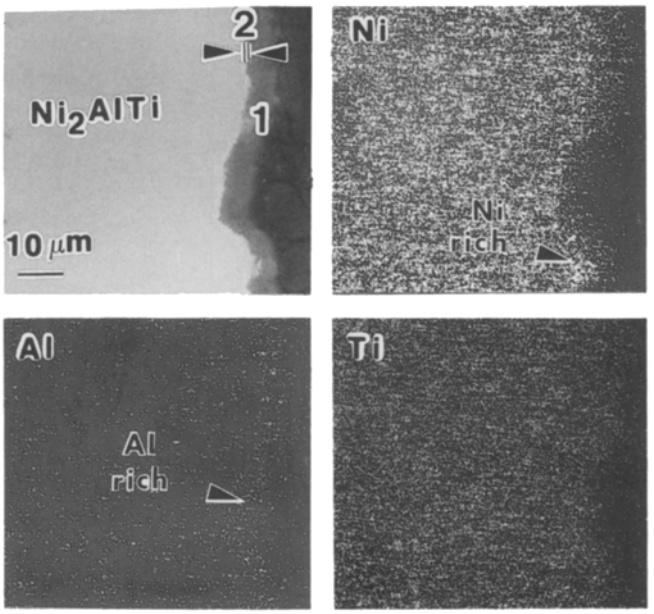

Figure 1 Back-scattered electron image and X-ray mapping of bulk Ni_2AlTi oxidized at 1200° C for 1 min, showing (1) an external oxide layer ($NiO + TiO_2 + Al_2O_3$), and (2) a Ni_3Ti layer.

3. Results

3.1. Oxidation of bulk Ni_2AlTi

3.1.1. Scanning electron microscopy

The back-scattered electron image (BEI) and X-ray mappings of the bulk sample oxidized at 1200° C for 1 min were shown in Fig. 1. A dark oxide layer and beneath it a thin bright layer were recognized on the surface. EDX showed some concentration of nickel, titanium and aluminium elements in the dark oxide layer which was later identified as oxide aggregates of $NiO + TiO_2 + Al_2O_3$ by X-ray diffraction. The thin bright layer is nickel-rich and was later identified to be Ni_3Ti phase by X-ray diffraction. No apparent duplex structure can be observed in this external oxide layer, although Al_2O_3 was formed in the initial stage of oxidation as indicated by aluminium-mapping (Fig. 1) and X-ray diffraction of oxidized powder.

Further oxidation at 1200° C (5 to 30 min) resulted in an intermediate layer between the external oxide layer and Ni_3Ti layer as shown representatively by the 10 min specimen in Fig. 2. This intermediate layer consists of an island-like bright phase and dark oxide phases in BEI. The bright phase is depleted of aluminium and has a counts ratio of Ni : Ti larger than that of Ni_2AlTi substrate by EDX analysis, and was later found to be Ni_3Ti alloy by X-ray diffraction. The dark oxide particles were generally too small to be analysed unambiguously by EDX technique. However, aluminium-rich oxide was still recognized and identified by X-ray diffraction to be $Al_2O_3 + NiAl_2O_4$ aggregates. Slight amount of $NiTiO_3$ (gray phase on BEI, arrow) which reflects more electrons than the aluminium-bearing oxides was also detected by X-ray diffraction.

3.1.2. X-ray diffraction

The oxide aggregates in the external oxide layer of the representative specimen oxidized at 1200° C for 30 min are mainly $NiAl_2O_4$ [12] and $NiTiO_3$ [13] by X-ray diffractogram of the outer surface. Slight diffraction intensity of Al_2O_3 [14] was contributed in part from the intermediate layer. After removal of about 10 μm of the outer layer, the diffraction lines of Ni_3Ti [15]

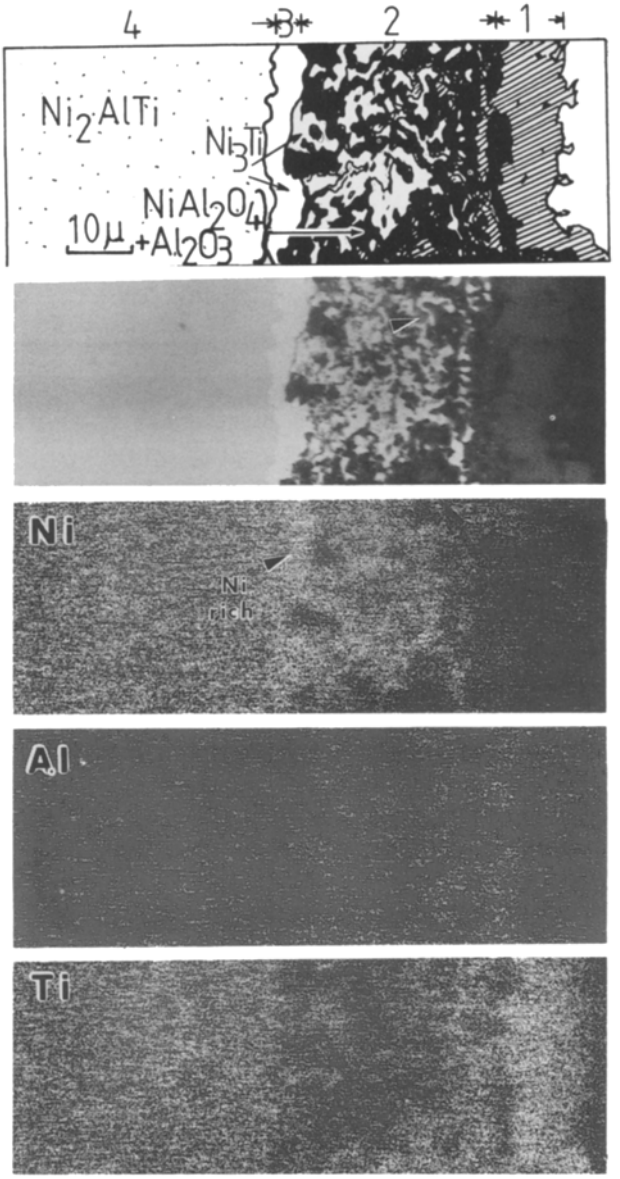

Figure 2 Back-scattered electron image, X-ray mapping and schematic indexing of bulk Ni_2AlTi oxidized at 1200° C for 10 min, showing (1) external oxide layer containing $NiAl_2O_4$, $NiTiO_3$, and small amount of Al_2O_3 (2) internal precipitation layer, (3) Ni_3Ti layer, and (4) substrate.

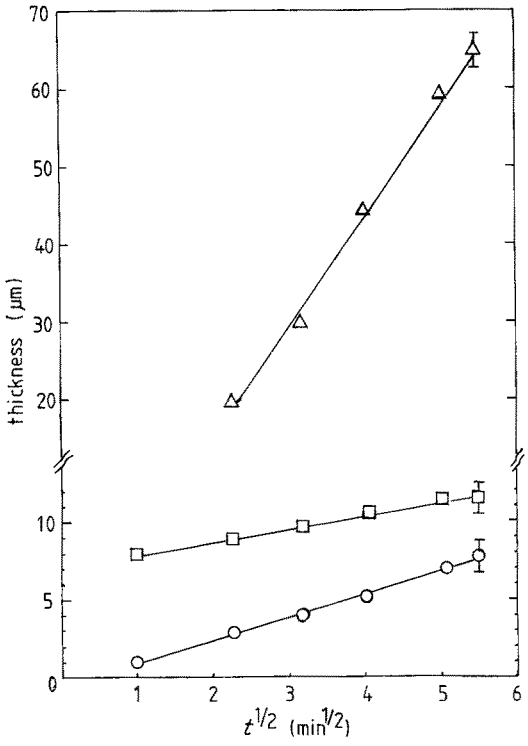

Figure 3 Parabolic plot of various layers formed at 1200° C. (□ external oxide layer, $K = 0.9$; △ internal precipitation layer, $K = 13.7$; ○ Ni_3Ti layer, $K = 1.6$).

showed up besides those of the three oxide phases which showed a decrease in intensity (especially $NiTiO_3$). The diffraction intensity of Ni_3Ti continued to increase, whereas those of oxides decrease gradually with further removal of the oxide layers.

3.1.3. Parabolic rate constant

The thickness of each layer was measured by making at least 10 observations on a given specimen (Table I). The layer thickness formed at 1200° C plotted against the square root of time in Fig. 3 and the parabolic rate constant, k, for the external oxide layer, intermediate layer and Ni_3Ti layer estimated to be 0.9, 13.7 and 1.6 $\mu m\,min^{-1/2}$ respectively. The intermediate layer and the Ni_3Ti layer were not formed for specimens oxidized at 900° C for up to 16 min.

3.2. Oxidation of Ni_2AlTi powder

The sequence of formation of various oxides was studied by X-ray diffraction and represented by the powder specimens oxidized at 1200° C for various times. Mechanical grinding of Ni_2AlTi powder did not introduce any other detectable phase. Isothermal oxidation at 1200° C for 5 sec, produced a significant amount of NiO [16] and TiO_2 [17]. The diffraction

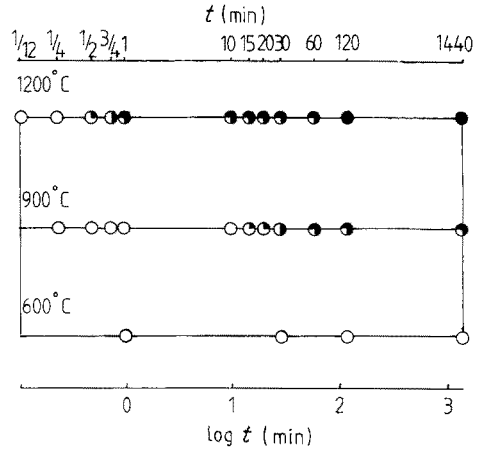

Figure 4 Existence diagram of oxides on Ni_2AlTi powder, notations of oxides are NiO (N), TiO_2 (T), Al_2O_3 (A), $NiTiO_3$ (NT), $NiAl_2O_4$ (NA). (○ N + T, ◔ N + T + A, ◑ N + T + A + NT, ◕ N + T + A + NT + NA, ● NT + NA).

lines of Al_2O_3, $NiTiO_3$, $NiAl_2O_4$ showed up after 30 sec, 45 sec, 1 min respectively. Further oxidation from 1 to 60 min resulted in the increase of the diffraction intensities of $NiTiO_3$ and $NiAl_2O_4$ and the decrease of the other phases. Oxidation for 2 to 24 h, $NiTiO_3$ and $NiAl_2O_4$ were the only remaining oxides on the X-ray diffractogram.

The results of X-ray diffraction of the oxide structure in the powder oxidized at 600, 900 and 1200° C were summarized in Fig. 4, which showed the types of oxides as a function of oxidation temperature and time. From Fig. 4 it can be deduced that NiO and TiO_2 were formed almost instantaneously in the early stage of oxidation, irrespective of oxidation temperature. Further oxidation at 900 and 1200° C produced Al_2O_3. The oxide of NiO then reacted with TiO_2 to form $NiTiO_3$ and the later the reaction of NiO and Al_2O_3 to form $NiAl_2O_4$ also occurred. The reaction of NiO + TiO_2 + Al_2O_3 to form $NiTiO_3$ and $NiAl_2O_4$ was almost complete within 2 h at 1200° C, but was incomplete at 900° C for 24 h. Throughout the time period studied, only NiO and TiO_2 were formed at 600° C.

4. Discussion

4.1. Initial stage oxidation and chemical reactions

Oxidation of bulk Ni_2AlTi specimens indicated a mixture of NiO, TiO_2 and Al_2O_3 were formed at the outer surface in the early stage (Fig. 1). Oxidation of Ni_2AlTi powder (Fig. 4) also indicated of NiO and TiO_2 were formed in the initial stage of oxidation. The absence of NiO and TiO_2 phases in powders oxidized at 1200° C for more than 120 min (Fig. 4) suggested they were

TABLE I Thickness of various layers in isothermally oxidized Ni_2AlTi

t (min)	External layer (μm)		Intermediate layer (μm)		Ni_3Ti layer (μm)	
	1200° C	900° C	1200° C	900° C	1200° C	900° C
1	8	–	–	–	1	–
5	9	5	20	–	3	–
10	10	8	30	–	4	–
16	11	9	45	–	5	–
25	~12	~10	60	–	7	1
30	12	10	65	–	8	2

transient phases, similar to the transient oxides of NiO and $NiCr_2O_4$ in the transient oxidation stage of Ni–Cr alloy [18, 19]. Besides oxidation of the alloy, a chemical reaction also occurred as indicated by the formation of $NiTiO_3$ and $NiAl_2O_4$ at the expense of the constituent oxides (Fig. 4). In a preliminary study acetates of nickel and aluminium were calcinated and ball-milled with TiO_2 additive to form a mixture of $2NiO + \frac{1}{2}Al_2O_3 + TiO_2$, then die-pressed and sintered at 1600° C for 4 h. The X-ray diffraction study indicated that the sintered discs also consisted of $NiTiO_3$ and $NiAl_2O_4$. The reaction between Al_2O_3 and TiO_2 to form Al_2TiO_5 was not detected.

4.2. Sesquioxide layer

According to Pettit [20] and Giggins and Pettit [21], the oxidation in the nickel-rich end of the nickel–aluminium–chromium system depends on the concentrations of aluminium and chromium. It was suggested by Giggins and Pettit [21] that during the initial stage of oxidation, an outer layer containing RO (R represents cations) and R_3O_4 with an R_2O_3 phase in the inner area was formed. If the content of aluminium and chromium is large enough, as in the aluminized coating on René 80 [11], a continuous R_2O_3 layer will form and subsequent oxidation is dominated by the outward diffusion of aluminium and chromium rather than by the inward diffusion of oxygen [21]. The area beneath the R_2O_3 layer will be depleted of aluminium and chromium. For the formation of a continuous Al_2O_3 layer the aluminium content must be more than 15 wt % in NiAl alloy, [20], but only 5 to 6 wt % Al is required if minor amount of chromium (4 to 5 wt %) is added [3]. It is not certain how much aluminium is necessary to form a continuous Al_2O_3 layer in nickel-rich Ni–Al–Ti alloy. The aluminium content in Ni_2AlTi (14 wt % Al) was probably not enough to form a continuous layer of Al_2O_3 as our results showed no evidence of it. However, an aluminium-depleted zone (Ni_3Ti layer) beneath the intermediate layer was still observed which indicated that aluminium diffused outward to form $NiAl_2O_4$ and Al_2O_3, though not a continuous layer.

4.3. Internal precipitation layer

The intermediate layer is similar to the internal precipitation layer found in dilute γ-Ni–Al alloys (nickel with up to 4 wt % Al), with or without a small additions of tantalum or hafnium [22]. The depletion of aluminium below the intermediate layer and an enrichment in the form of oxides within the intermediate layer suggested that the growth was controlled by simultaneous outward aluminium and inward oxygen diffusion. The coalesence of the rod-like oxides resulted in the development of a continuous Al_2O_3 film at the front of the intermediate layer [22]. However, no apparent continuous Al_2O_3 film or rod-like Al_2O_3 precipitates were recognized in the present specimens on SEM photographs. Detailed microstructural observations on deeply etched specimens prepared by partial selective alloy dissolution are required to examine clearly the morphology of internal precipitates.

TABLE II Experimental data for intermediate-layer growth rate constant, k, for Ni–Al alloys oxidized at 1200° C

Alloy composition	Al atom fraction, N_{Al}	k ($\times 10^4$ cm sec$^{-1/2}$)
Ni–0.5 wt% Al*	0.011	1.94
Ni–2 wt% Al*	0.043	0.83
Ni–4 wt% Al*	0.083	0.61
Ni–2 wt% Al–1 wt% Ta*	0.043	1.04
Ni–2 wt% Al–1 wt% Hf*	0.043	1.04
β-NiAl	0.519	0.01
Ni_2AlTi (present work)	0.25	1.8

*Dilute γ-NiAl alloy after ref [22], Hindam and Whittle 1983. β-NiAl calculated from parabolic growth plot of Al_2O_3 scale [23], Jedlinski and Mrowec 1987.

4.4. Parabolic rate constant

Compared to β-NiAl, Ni_2AlTi has a lower activity of aluminium, therefore less Al_2O_3 can be formed. The retrograded metal phase in Ni_2AlTi was Ni_3Ti which also contained less aluminium than Ni_3Al or Ni_2Al found in retrograded β-NiAl [5, 6]. Furthermore a significant amount of TiO_2, which was known to deteriorate the oxidation resistance of René 80 [5, 11], was formed in the initial stage and subsequent stages of oxidation of Ni_2AlTi. The isothermal (1200° C) parabolic oxidation rate constant, k of Ni_2AlTi, β-NiAl [23] and dilute γ-NiAl alloy, either pure or containing tantalum or hafnium [22] were compiled in Table II. The k value of Ni_2AlTi is two orders of magnitude higher than that of β-NiAl and is close to those of dilute γ-NiAl alloy. It follows, therefore, that Ni_2AlTi is not good oxidation-resistant material for use in high temperature technology, although its creep strength is about three times that of β-NiAl [9]. According to Table II, the k value decreases, hence oxidation resistance improves, as the aluminium atom fraction N_{AL} increases in dilute γ-NiAl alloy [22]. Although the aluminium content of Ni_2AlTi is significantly richer than in dilute γ-NiAl alloy, the k values of both are about the same order of magnitude. The poorer-than-expected oxidation resistance for Ni_2AlTi was probably due to the formation of TiO_2 and $NiTiO_3$ which were absent in the oxidized Ni–Al alloy. The possible anisotropic thermal expansion of TiO_2 (tetragonal structure) and $NiTiO_3$ (hexagonal structure), could also deteriorate the oxidation resistance.

5. Conclusions

The isothermal oxidation process of Ni_2AlTi alloy in the temperature range of 600 to 1200° C was studied by SEM and X-ray diffraction. Only NiO and TiO_2 were formed at 600° C up to 24 h. Unless specified, the following conclusions are common to oxidation at 900 and 1200° C.

(1) Transient oxides, NiO and TiO_2 were formed in the initial stage on the outer surface.

(2) Subsequent oxidation was dominated by outward diffusion of aluminium resulting in the formation of Ni_3Ti layer beneath an intermediate layer containing mainly $Al_2O_3 + NiAl_2O_4$ aggregates, $NiTiO_3$ and Ni_3Ti.

(3) In the late stage of oxidation, formation of

$NiTiO_3$ and $NiAl_2O_4$ at the expense of constituent oxides occurred.

(4) The oxidation rate of Ni_2AlTi is about the same order of magnitude as the dilute γ-NiAl alloy at 1200° C.

Acknowledgements

Thanks are due to Dr D. Gan for comments and Mr S. L. Hwang for preparing the Ni_2AlTi sample. Several oxidation runs were made by Mr S. Chen. This work was supported by National Science Council of Taiwan, R.O.C. under contract number NSC76-0405-E110-07.

References

1. G. W. GOWARD, D. H. BOONE and C. S. GIGGINS, *ASM Trans. Quart.* **60** (1967) 228.
2. T. K. REDDEN, *Trans. TMS-AIME* **242** (1968) 1695.
3. G. W. GOWARD, *J. Metals* **22** (1970) 31.
4. G. W. GOWARD and D. H. BOONE, *Oxid. Metals* **3** (1971) 475.
5. C. C. LIN, D. TU, P. SHEN and D. GAN, *Chinese J. Mater. Sci.* **16A** (1984) 74.
6. M. J. TSAI and P. SHEN, *Mater. Sci Eng.* **83** (1986) 135.
7. P. SHEN, D. GAN and C. C. LIN, *ibid.* **78** (1986) 163.
8. P. SHEN, C. C. CHOU, M. J. TSAI and C. C. LIN, *ibid.* **87** (1987) 145.
9. P. R. STRUTT, R. S. POLVANI and J. C. INGRAM, *Metall. Trans. A* **7** (1976) 23.
10. M. YAMAGUCHI, Y. UMAKOSHI and T. YAMANE, *Phil. Mag. A* **50** (1984) 205.
11. C. C. LIN, M. S. THESIS, National Sun Yat-Sen University (1983).
12. JCPDS file 10-339.
13. JCPDS file 17-617.
14. JCPDS file 10-173.
15. JCPDS file 5-723.
16. JCPDS file 4-835.
17. JCPDS file 21-1276.
18. B. CHATTOPADHYAY and G. C. WOOD, *J. Electrochem. Soc.* **117** (1970) 1163.
19. A. TAKEI and K. NII, *Trans. JIM* **17** (1976) 211.
20. F. S. PETTIT, *Metall. Trans.* **239** (1967) 1296.
21. C. S. GIGGINS and F. S. PETTIT, *J. Electrochem. Soc.* **118** (1971) 1782.
22. H. HINDAM and D. P. WHITTLE, *J. Mater. Sci.* **18** (1983) 1389.
23. J. JEDLINSKI and S. MROWEC, *Mater. Sci. Eng.* **87** (1987) 281.

Received 7 July
and accepted 18 November 1988